Desalination and Water Treatment
www.deswater.com

doi:10.5004/dwt.2017.20321

68 (2017) 199–210
March

Sorption and separation study of praseodymium and cadmium by magnetic bentonite. Factorial design optimization

Ousama Belyouci, Mohamed Amine Didi*

Laboratory of Separation and Purification Technologies, Department of Chemistry — Faculty of Sciences, Box 119, Tlemcen University — 13000, Algeria, Tel. +213 552383970, email: Belyouci@yahoo.com (O. Belyouci), Tel. +213 552639237, Fax: +213 43213198, email: madidi13@yahoo.fr (M.A. Didi)

Received 13 June 2016; Accepted 4 November 2016

ABSTRACT

Magnetic bentonite was successfully synthesized by incorporating ferrofluids based on maghemite nanoparticles (γ-Fe_2O_3) and bentonite. The capacity of magnetic particles to remove praseodymium and cadmium ions from aqueous media was investigated. A magnetic adsorbent can be quickly separated from a medium by a simple magnetic process. Based on these properties, some parameters were studied to assess the performance of maghemite nanocomposite clay in removing and separating ions from a medium. Parameters such as the initial pH, dosage of adsorbent and contact time have been examined in order to find the optimum adsorption conditions. The results revealed that 74.32% and 15.06% of Pr (III) and Cd (II), respectively, were extracted within 20 min at pH 6.5. The separation was optimized according to a complete factorial design 2^3. The individual effects, as well as the interactions between variables were studied. Student and Fisher's tests indicated that the pH and initial metal ion concentration are certainly the most influential parameters. The experimental adsorption isotherm data were analyzed using Langmuir, Freundlich and Tempkin isotherm equations. Freundlich isotherm showed a better fit for praseodymium and cadmium adsorption. The optimal extraction by magnetic bentonite was obtained after six cycles with 0.01 g of adsorbent, and two cycles with 0.05 g of adsorbent.

Keywords: Praseodymium; Cadmium; Factorial design; Maghemite; Sorption; Selectivity

1. Introduction

According to the International Union of Pure and Applied Chemistry (IUPAC), rare earth elements (REE) are formed by 17 similar metallic elements including scandium (Sc), and Yttrium (Y). Praseodymium (Pr) is one of the most abundant rare earth elements [1].

Recently potential applications of rare earth elements in various strategic fields have become more attractive [2]. All rare chemicals have comparable properties. Praseodymium is one of the rare chemicals that can be found in home equipment such as color televisions, fluorescent lamps, energy saving lamps and glasses [3]. The use of praseodymium is still growing, due to the fact that it is well-suited for producing pigments, materials with higher electrical conductivity and catalyzers [4]. Despite its wide range of applications in various areas, praseodymium may still be harmful to human health [5].

Owing to the high commercial value of rare earths elements, in various important fields, and the hazards induced by their presence in the environment, the separation and recovery of those elements from different media has becomes important. Therefore, a lot of research has been done to develop successful solvent extraction and ion exchange processes to separate rare earths from aqueous solutions [6,7].

*Corresponding author.

A large number of studies have been conducted to develop cheaper and effective adsorbents of mineral, organic or biological origin, zeolites [8], industrial by-products, agricultural wastes [9], and adsorbents based on biopolymers such as cellulose [10]. Even though these adsorbents have proved to be very effective in removing pollutants from wastewater [11,12], the development of new adsorbents and new removal systems is still very essential.

Interest in maghemite nanoparticles covers many areas of science and technology. They are particularly used in many biomedical and industrial applications; they are currently applied in DNA purification, drug delivery, magnetic membranes, catalysis and other applications [13]. Maghemite is suitable for the extraction of hazardous substances from wastewaters. It is used in magnetic separation techniques which aim to provide a more effective, less expensive, easier way to remove hazardous metals from wastes [14]. Considering their wide applications and unique characteristics, magnetic nanoparticles, particularly maghemite grafted with bentonite, have received much attention in environmental applications. They may be used in the adsorption of chemicals and separation of contaminants [15,16]. Montmorillonite-rich materials, such as bentonites, exhibit highly interesting properties, as well as high specific surface area, cation exchange capacity (CEC), porosity, and tendency to retain water or other polar and non-polar compounds; it is also an inexpensive operation [17]. Over the last few years, magnetic separation has become a promising new environmental purification technique due to lack or insufficient production of flocculants. This technique allows treating large amounts of wastewater within a short time [18,19]. In addition, it is an excellent adsorbent which should have more surface area; it needs a very short time to reach equilibrium.

In this work, the adsorption features of bentonite together with the magnetic properties of iron oxides have been combined into one composite to produce a magnetic adsorbent. Due to the presence of the metal component, bentonite can rapidly and easily be separated from water by simple application of an external magnetic field, which is a cost effective technique. It is therefore proposed to separate Pr (III) from binary systems containing cadmium Cd (II) and Pr (III) 1:1, knowing that cadmium is one of the most toxic and carcinogenic heavy metals capable of causing serious environmental and health problems [20]. It is released to the environment from point sources, such as metal mining discharges, as well as metal plating, battery, and paper industries [21].

The effects of various parameters, including contact time, initial pH, initial concentrations of Praseodymium and cadmium and the amount of adsorbent, on separation process, were used in the factorial design to optimize the procedure. Langmuir, Freundlich and Temkin isotherm models were studied.

2. Materials and methods

2.1. Reagents

Praseodymium and cadmium solutions at 10^{-3} M were prepared by dissolving of praseodymium nitrate hexahydrate 0.218 g and 0.183 g cadmium iodide in 500 mL of distilled water (purchased by Sigma-Aldrich). The initial pH of the sample solutions was adjusted by using dilutes HCl or NaOH (from Sigma-Aldrich). Arsenazo III 10^{-3} M (from Fluka) was prepared by dissolving 0.0820 g in absolute ethanol. Bentonite used in this study is a montmorillonite-rich material originating from Hammam Boughrara deposit (Maghnia, Algeria), and supplied by ENOF Ltd. (Algeria), sodium thiosulfate pentahydrate (from Sigma-Aldrich). For magnetic nanoparticles synthesized, $FeCl_2{\cdot}4H_2O$ (from Sigma-Aldrich), $FeCl_3{\cdot}6H_2O$ (from Panreac), NH_4OH (from Sigma-Aldrich), HNO_3 and $Fe(NO_3)_2$ (fromSigma-Aldrich) were used.

2.2. Apparatus

The separation of Pr (III) from Cd (II) was studied by the batch process using a stirring vibrator (Haier model). pH measurements were performed with a pH meter using a combined electrode mark (Adwa). X-Ray fluorescence spectroscopy of dried Bentonite were performed using Philips PW 3710.Thermogravimetric analyses of samples (TGA) were performed using a SDT Q600 thermogravimetric analyzer at a heating rate of 20°C/min under nitrogen atmosphere, Tlemcen–Algeria. A magnet for the recovery of the magnetic bentonite in the aqueous phase was used. Maghemite is magnetic with magnetization, σ, was performed using a Teslameter M-Test LL.

Samples containing metal ions were analyzed by spectrophotometer (Analytik Jena Specord 210 Plus) with Arsenazo III as ligand; the concentrations of Cd (II) in the aqueous phase were determined using an atomic adsorption spectrophotometer (Perkin Elmer Pinnacle 500), Tlemcen-Algeria.

2.3. Extraction procedure

All the adsorption experiments were carried out at room temperature (20 ± 1°C) in a typical procedure; 0.01 g of the magnetic bentonite was added to 5 mL of solute concentration, at pH value 6.5 ± 0.1, in 250 mL Erlenmeyer flasks under vigorous Stirring. After adsorption, the sorbents were separated with a magnet, the concentrations of Pr (III) was determined by UV-Visible spectrometer at sample pH adjusted to 2.5 and mixed with 150 µL Arzenazo III solution, and Cd (II) in the aqueous phase was determined using an atomic adsorption spectrophotometer.

The adsorption capacity q_e (mg/g), was calculated using:

$$q_e(mg/g) = (C_0 - C_e)\cdot V \cdot M / m \quad (1)$$

where C_0 and C_e are initial concentration and equilibrium concentration (mol/L), respectively, M is the molecular weight of metal ion and m is the masse of adsorbent (g).

The adsorption efficiency is calculated as follows:

$$\text{Extraction Yield (\%)} = \frac{C_0 - C_{eq}}{C_0}\cdot 100 \quad (2)$$

2.4. Preparation of magnetic Ferrofluid

The magnetic ferrofluid was obtained by dispersion of maghemite in an aqueous solution. At the beginning, magnetite (Fe_3O_4) was synthesized by coprecipitation of a stoichiometric mixture of ferrous and ferric chlorides in an ammonium hydroxide solution. Then, the black precipitate was acidified by nitric acid and oxidized into maghemite (γ-Fe_2O_3) at 90°C, with iron (III) nitrate. The maghemite particles obtained were precipitated by means of acetone, and then dispersed into water leading to an acid ionic ferrofluid (pH 2.0). After this step, nanoparticles were positively charged with nitrate as counter-ions [22,14]. Maghemite has magnetization σ equal to 102 J T^{-1} kg^{-1} [23].

2.5. Bentonite purification

The natural bentonite used in this study was obtained from deposits in the area of Maghnia, Algeria. The chemical composition of natural bentonite was determined by X-ray fluorescence spectroscopy and is summarized in Table 1. The mineralogical analysis showed that the native crude clay mineral contains preponderantly montmorillonite (86 wt.%); the clay composition also includes quartz (10%), cristobalite (3.0%) and beidellite (less than 1%).

For the purification of natural bentonite, 120 g was dispersed in 1.5 L of distilled water; after agitation during 15 min, a buffer solution of sodium citrate (pH 7.3) was added. The mixture was heated under agitation at 75°C during 20 min and then, 15 g of sodium thiosulfate ($Na_2S_2O_4$) was slowly added. After 15 min under agitation, the mixture was cooled and centrifuged at a rotational speed of 6000 rpm (Centrifugal type JA 10) for 15 min. The solid recovered was washed two times with HCl 0.05 M (1.5 L) during 3 h [24]. The chemical composition of purified bentonite was determined by X-ray fluorescence spectroscopy and summarized in Table 1.

X ray Difractograms (XRD) of natural bentonite and purified bentonite are shown in Fig. 1. The purification is confirmed by the loss of some impurities, especially quartz at q = 26.8. The conjugation of some peaks at q = 5.7 and 29, then the appearance of new rays initially masked by quartz at q = 15 and 17°.

2.6. Preparation of magnetic bentonite

An amount of 100 mL of the ferrofluid, of black color, and 18 g of purified bentonite, a white powder, were mixed at room temperature. The mixture was stirred for 60 min, and then decanted onto magnetic plates. The brown precipitate obtained is due to the excess of magnetic particles. Next, the precipitate was dried in an oven at 50°C for 24 h, then ground and passed through a 0.24 mm sieve.

2.6.1. Thermogravimetric analysis

Thermogravimetric analysis of maghemite showed a weight loss due to water vapor of approximately 0.9% at temperatures lower the 100°C. In the temperature range 120–180°C it is observed a weight gain of ca. 0.3% which is probably related to the oxidation of small amounts of Fe^{2+} present in the sample. For aged samples, this weight gain is not observed, suggesting that this Fe^{2+} is slowly oxidized by air at room temperature.

TGA for the dried purified bentonite pattern, 1.128% weight-loss was checked at the temperature range of 59.61–123.15°C, 1.982% weight-loss appeared at 472.48–591.97°C and 1.708 % weight-increase appeared at 873.61–880.48 due to the absorption of the nitrogen.

Thermogravimetric analysis of the bentonite : Fe oxide composite (Fig. 2) showed H_2O loss of 6.40% at the temperature range of 39.00–121.43°C, 1.187% weight-loss appeared at 171.24–231.34°C, a weight decrease of approximately 1.10% observed for the Bentonite: Fe oxide composite between 301.82–396.74°C is probably related to dehydroxylation of the Fe oxide present in the composite and 1.50% weight-loss appeared at 567.71–664.01°C likely related to the clay showing on the dehydroxylation of the composite. Upon heating, clay minerals usually become dehydroxylated and their structure break down at temperatures that are often characteristic for individual species.

3. Results and discussion

In this study different parameters were examined: effect of contact time, effect of initial pH, initial concentrations of praseodymium and cadmium, effect of initial amount of adsorbent and the effect of ionic strength.

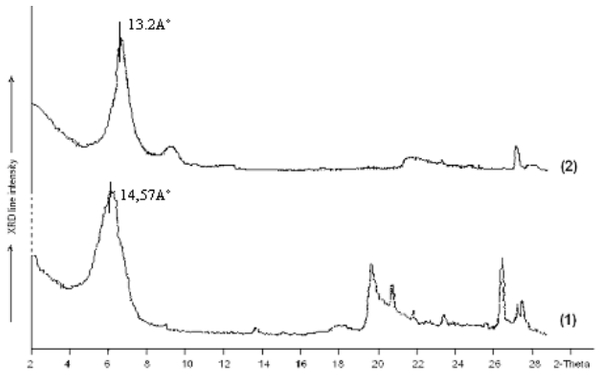

Fig. 1. XRD Difractograms of natural Bentonite[1] and purified Bentonite[2].

Table 1
Elemental composition of natural Bentonite and purified Bentonite

Composition	SiO_2	Al_2O_3	Fe_2O_3	MgO	K_2O	CaO	TiO_2	Na_2O	As	LI
% (weight of natural bentonite)	62.4	17.33	1.2	3.56	0.8	0.81	0.2	0.65	0.05	13.0
% (weight of purified bentonite)	64.7	18.1	0.95	2.66	0.8	0.61	0.2	1.93	0.05	10.0

LI: Loss on ignation at 900°C.

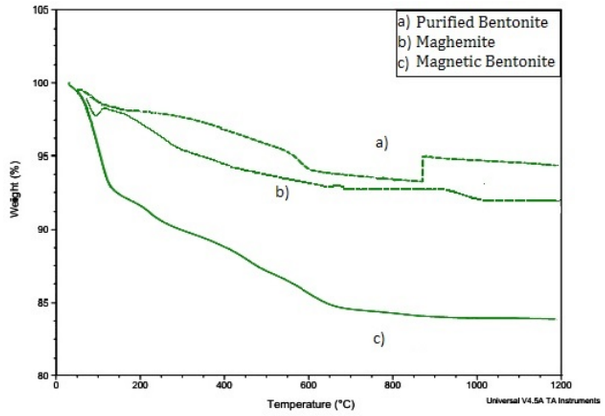

Fig. 2. Thermogravimetric analyses in air for the (a) The purified bentonite (b) maghemite (γ-Fe_2O_3) and (c) magnetic bentonite.

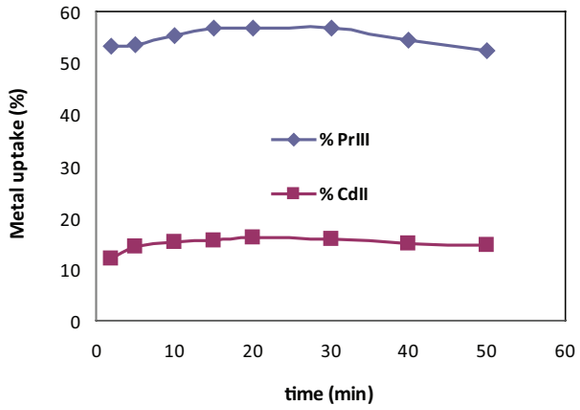

Fig. 3. Effect of contact time on removal of Pr(III) and Cd(II) by magnetic bentonite. $[Pr\ (III)]_0 = [Cd\ (II)]_0 = 10^{-3}$ mol·L^{-1}, w = 0.01 g, V = 5 mL, Ø = 250 rpm.

3.1. Effect of contact time

The effect of contact time in adsorption sufficiency of praseodymium and cadmium was analyzed kinetically over a range of 2–50 min. The reaction was stimulated by shaking with magnetic bentonite at 250 rpm at 20°C with initial metal solution of pH 6.5.The initial solution concentration was 10^{-3} mol·L^{-1} for Pr (III) and Cd (II), while amount of adsorbent was 0.01 g/5 mL. Adsorption capacities were measured as a function of time (shown in Fig. 3). It was observed that removal of metal ions was rapidly achieved, within a short period of 20 min. That is probably due to the large surface of magnetique bentonite being available at the beginning. Adsorptions onto our adsorbent within short time of 20 min become interesting for liquid-solid extraction, comparing to Core–nanoshell magnetic composite material with 80 min equilibrium time [25].

3.2. Effect of pH

The separation of metal ions from aqueous solution by adsorption was studied over a pH range from 2.2 to 11.0, while maintaining the other parameters constant. HCl and NaOH solutions were used to adjust system pH. It was observed from Fig. 4, that the metal ion sorption process is dependent on the initial pH of the solution and the amount of metal ions sorbed increased with the increase of the pH value. The zero point of charge (ZPC) of maghemite is at pH of 6.6. At lower values, a poor adsorption is observed because the metal ion uptake was inhibited in this acidic medium and this can be attributed to a pronounced impact of electrostatic repulsion between positively charged Pr(III), Cd(II) and positive charged surface of maghemite below the pH of (ZPC) [26]. Primordially, Pr(III) and Cd(III) exists in their ionic forms between pH 2.0 and 6.5. A remarkable removal efficiency of Pr(III) increase with decrease of pH to 6.5 but Cd(II) adsorbs lesser than Pr(III) and the difference on adsorption capacity keeps almost constant. This result shows the occurrence of competition phenomena between praseodymium and cadmium on adsorption in actives sites of magnetic bentonite, which the maghemite is not charged at pH 6.6. Above the pH of ZPC, the particle surface processes an overall negative charge while the dominant species Fig. 5 of Praseodymium were Pr^{3+} and $Pr(OH)^{2+}$ and dominant species of Cadmium Cd^{2+} , CdI^{+} and $Cd(OH)^{+}$ and thus under basic conditions electrostatic attraction exists and high adsorption is observed.

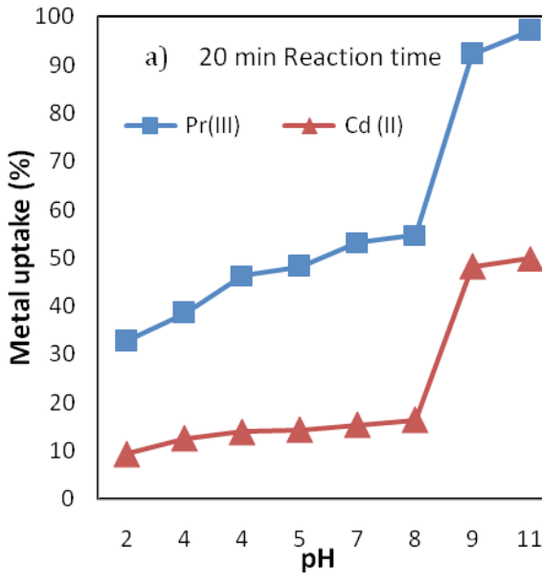

Fig. 4. Effect of pH on Pr (III) and Cd (II) adsorption. $[Pr\ (III)]_0 = [Cd\ (II)]_0 = 10^{-3}$ mol·L^{-1}, $w_{(\text{magnetic bentonite})}$= 0.01 g, Ø = 250 rpm.

3.3. Effect of initial amount of adsorbent

One of the most important parameters is the adsorption dosage. The number of sites available for adsorption of metal ions depends on the amount of adsorbent used. The influence of the amount of adsorbent on the adsorption yield was determined at the initial metal ion concentration of 10^{-3} mol·L^{-1} and at pH 6.5. The results shown in Fig. 6 indicate that the adsorption efficiency increased from 37.8–74.3% for praseodymium, and from 12.1–15.1%

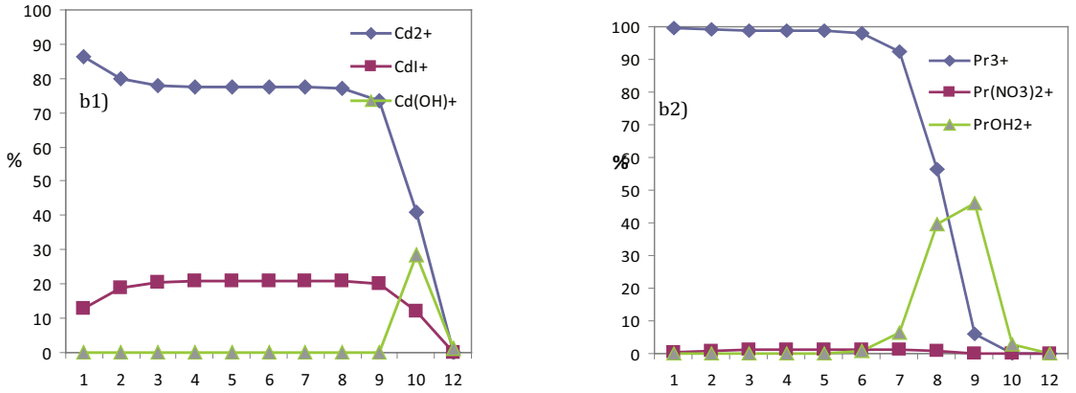

Fig. 5. Distribution diagrams using Medusa and Hydra programs [27]. (b1) $[Cd(II)]_0 = 10^{-3}$ M, $[I^-] = 2 \cdot 10^{-3}$ M, pH = 1–12; (b2) $[Pr(III)] = 10^{-3}$ M, $[NO_3^-] = 3 \cdot 10^{-3}$ M. pH = 1–12.

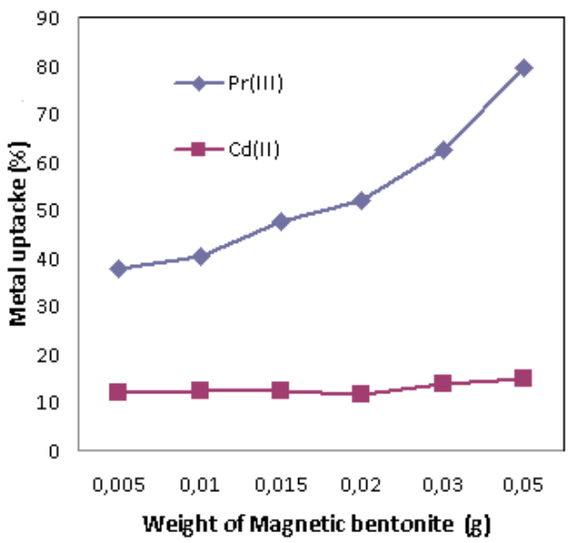

Fig. 6. Effect of the initial weight of magnetic bentonite on Pr (III) and Cd (II) adsorption. $[Pr(III)]_0 = [Cd(II)]_0 = 10^{-3}$ mol·L^{-1}, t = 20 min, V = 5 mL, Ø = 250 rpm, pH_i = 6.5.

for cadmium, when the adsorbent doses were raised from 0.005–0.05 g. It is observed that the adsorption of praseodymium increased is due to an increase in the surface area of adsorbent [28], but the adsorption increase of cadmium is smaller than that of praseodymium due to the phenomenon of competition in the adsorption of metal ions in active sites. For the mixture (Pr (III) + Cd (II)), the results show that the effect of the adsorbent on the adsorption efficiency is very selective for praseodymium adsorption on magnetic bentonite.

3.4. Effect of metals concentration

The influence of initial metal concentration on adsorption efficiency onto magnetic bentonite is shown in Fig. 7. It was carried out, at different initial concentrations of Pr(III) and Cd(II), from 0.2 mM to 1.0 mM, under the operating

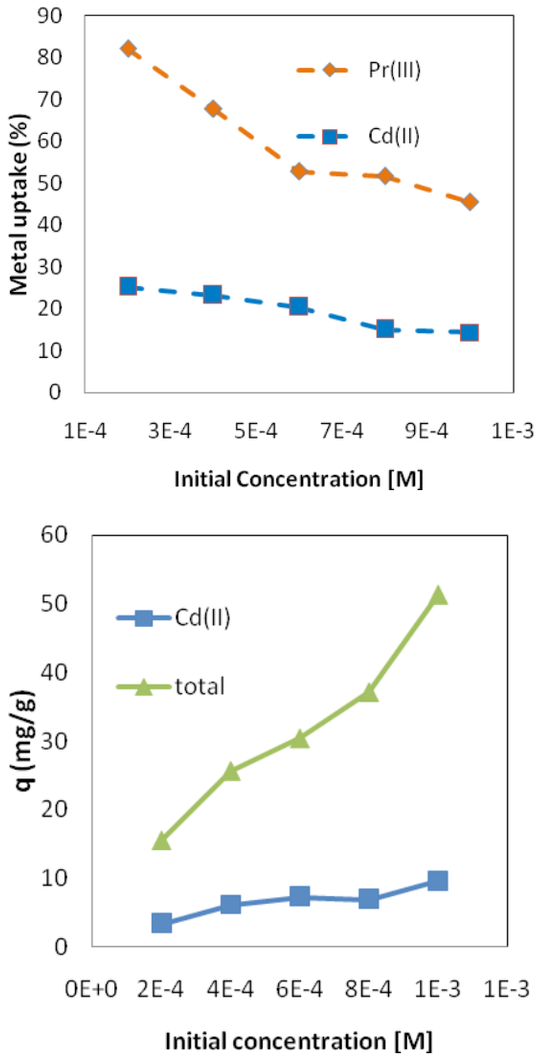

Fig. 7. Effect of the initial concentration on Pr (III) and Cd (II) adsorption by magnetic bentonite $w_{\text{magnetic bentonite}} = 0.01$ g, t = 20 min, V = 5 mL, Ø = 250 rpm.

pH of 6.5 and agitation 250 rpm within the equilibrium of 20 min. The adsorption efficiency increased with increasing metal ions efficiency until the saturation of available adsorption sites, the observed trend of percentage removal of metal ions was Pr (III) > Cd (II).

3.5. Adsorption isotherms

Langmuir, Freundlich and Temkin isotherm models were used in this study to establish the relationship between the amount of adsorbed metal onto our magnetic bentonite and its equilibrium concentration in aqueous system [29].

The Langmuir model assumes monolayer coverage of adsorbent surface, the global and linear form of Langmuir isotherm is given by the following equation:

$$\frac{q_e}{q_m} = \frac{K_L \cdot C_e}{1 + K_L C_e} \tag{3}$$

$$\frac{C_e}{q_e} = \frac{1}{q_m K_L} + C_e \frac{1}{q_m} \tag{4}$$

where C_e is equilibrium concentration of the adsorbate (mol·L^{-1}), q_m and K_L are Langmuir constants related to maximum of adsosrption capacity and energy of adsorption, respectively. The value of q_m and K_L can be obtained from the intercept and slope of the plot of C_e/q_e versus C_e, as shown in Fig. 8b.

The Freundlich isotherm model applied to adsorption on heterogeneous surfaces with interaction between adsorbed molecules and it's not restricted to the formation of a monolayer. The equation can be described by the linearized form:

$$q_e = K_F \cdot C_e^n \tag{5}$$

$$Log q_e = Log K_F + n Log C_e \tag{6}$$

where K_F (mg·g^{-1}) and n are the Freundlich constants of the system indicate adsorption capacity and adsorption intensity, the value of K_f and n obtained from the intercept and slope of the plot of Log q_e versus Log C_e as shown in Fig. 8a.

Temkin isotherm describes the adsorption potentials of adsorbent and adsorbate and is given by the following equation:

$$q_e = a + n Log C_e \tag{7}$$

where C_e is the concentration of metal ions at equilibrium (mol/L), q_e is the amount of praseodymium and cadmium adsorbed per unit weight of adsorbent (mg/g), a and b are constants related to adsorption capacity and intensity of adsorption respectively and were calculated from the intercept and slope of the plot of q_e versus log C_e, Fig. 8c.

However the higher correlation coefficient obtained from Freundlich plot represented in (Table 2) compared to Langmuir plot Temkin and suggests multi layer coverage of the adsorbent by metals ions in system.

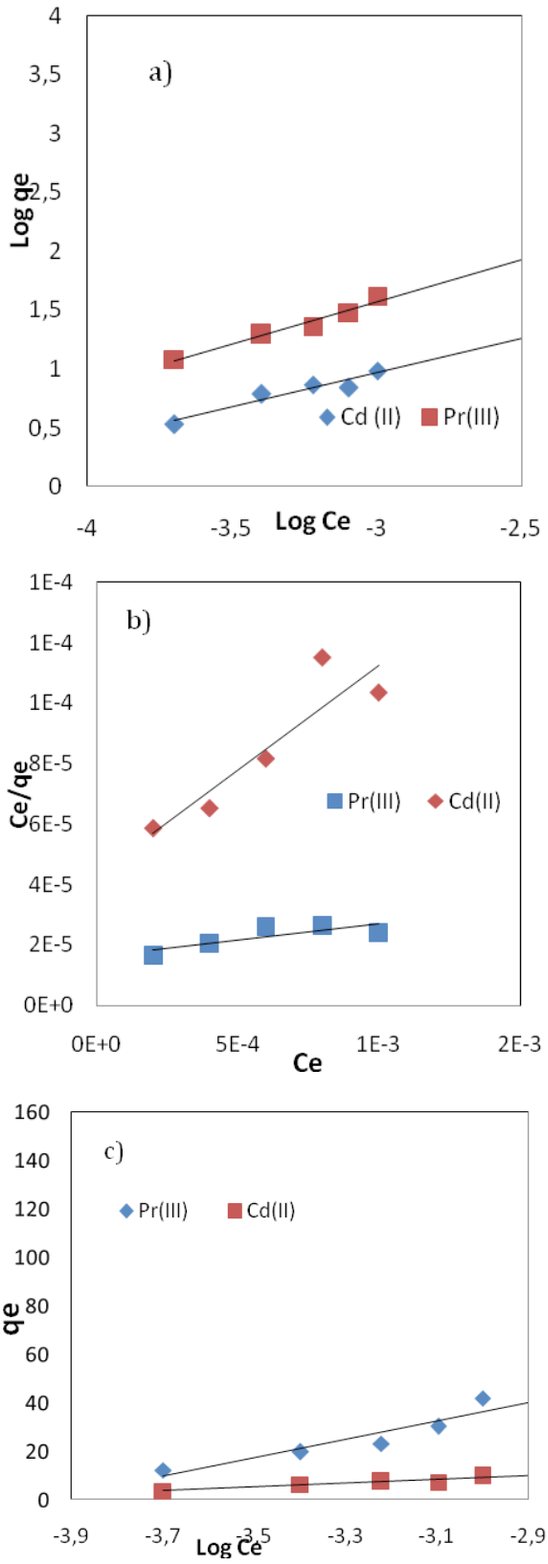

Fig. 8. (a) Freundlich isotherm illustrating the linear dependence of log q_e on log C_e, (b) Langmuir isotherm illustrating the linear dependence of C_e/Q_e on C_e, (c) Temkin isotherm illustrating the linear dependence of Q_e on log C_e.

Table 2
Isotherm parameters and correlation coefficient of Langmuir, Temkin and Freundlich; for Pr (III) and Cd (II) adsorption onto magnetique bentonite

	Freundlich			Langmuir			Temkin	
	K_f	n	R^2	q_m	K_L	R^2	b	R^2
Pr(III)	5292.97	0.71	0.9662	95.32	555.55	0.6268	37.87	0.8686
Cd(II)	516.29	0.58	0.9177	14.36	1740.94	0.8309	7.75	0.8955

For praseodymium, the sorption capacity of bentonite-γ-Fe_2O_3 (95.32 mg/L) was better that the sorption capacities with NiFeO (12.5 mg/L) and CuFeO (9.09 mg/L) [30].

3.6. Multi-component system adsorption kinetics of metal ions

Binary adsorption studies are important to assess the degree of interference posed by common metal ions present in water solution [31]. The effect of the ionic interactions on the adsorption may be represented by the ratio of the maximum adsorption capacity for one ion in the presence of the other ions, q_m, to the adsorption capacity for the same ion when it is present alone in the solution, q_0.

$\frac{q_m}{q_0} \succ 1$: synergism (the effect of the mixture is greater than that the individual adsorbents in the mixture).

$\frac{q_m}{q_0} = 1$: Non-interaction (the mixture has no effect on the adsorption of each of the adsorbents in the mixture).

$\frac{q_m}{q_0} \prec 1$: Antagonism (the effect of the mixture is less than that each of the adsorbents in the mixture).

Several factors were considered to correlate metal ion uptake with metal ions properties. Factors like (i) the electronegativity of the metal ion, (ii) electrostatic attrition due to charge to radius ratio, (iii) ability to form a metal hydroxide complex and (iv) suitable sites for adsorption on adsorbent are responsible for competitive adsorption of one metal ion over another. The hydrated radii of metal ions were 6.57Å for Pr (III) and 4.26Å for Cd (II). Thus, Cd (II) ions have higher accessibility to the surface and pores than Pr (III) cations, which leads to preferred adsorption of Cd (II). Pr (III) has a higher hydrated radii and molecular weight in comparison to Cd (II). It was observed from Table 2 that the Freundlich isotherm model showed the best fit for mono- and multi-component system compared to Langmuir and Temkin isotherm models.

3.7. Experimental design

Experimental design method is able to detect possible interactions with a reasonable number of experiments [31], in this investigation for quantification of the effects of three variables on the praseodymium and cadmium removal, a two level factorial design (low and high) of experiments was adopted. The variables studied were pH of solution (2.2, 11), initial metal concentration (2.10^{-4}, 10^{-3} mol·L^{-1}) and amount of adsorbent (0.005, 0.05 g), defined by the coded variables X_1, X_2 and X_3 respectively. If number of factors and levels increases, the number of experiments geometrically increases, the variables and levels for the study were given in Table 3.

Table 3
Factor levels used in the 2^3 factorial experiment design

Variable	Real values of coded levels	
	–1	+1
pH	2.2	11
Initial concentration [mol.L^{-1}]	2.10^{-4}	10^{-3}
Mass of adsorbent (g)	0.005	0.05

To evaluate the main effects of these three factors, their interactions, a 2^3 experiment factorial design with 8 runs experimental design was built, but totally 11 experiments were performed because three additional attempts at the central point (0, 0, 0) are required for estimating the average error in the value of each coefficient, on the basis of the random variance. The model is given in Eq. (8).

$$Y = a_0 + a_1X_1 + a_2X_2 + a_3X_3 + a_{12}X_1X_2 + a_{13}X_1X_3 + a_{23}X_2X_3a_{123}X_1X_2X_3 \quad (8)$$

where Y, is the predicted response (adsorbed metal ion amount); and X_j values (j = 1, 2, 3) represent the corresponding parameters in their coded forms. a_0 gives the average value of the results obtained for the adsorbed metal amount; a_1, a_2 and a_3 are linear coefficients shows the effect of pH of solution, initial metal concentration and amount of adsorbent respectively; a_{12}, a_{13}, a_{23} and a_{123} are the interaction coefficients shows the interacting effect of all three variables taken at a time, Fig. 9 show the coefficient values of the model, supposed to describe the individual effects of parameters, along with their possible interactions [32]. The values of regression coefficients determined are given in Table 4. Both of the low (–1) and high (+1) levels of every factor are compared with each other and the effects of each of the factor levels on the response are investigated according to the levels of other factors as shown in table. The equations for praseodymium and cadmium separation by adsorption were obtained from the trial runs and presented in Eqs. (9) and (10).

$$Y_{Pr} = 65.60 + 25.20X_1 - 2.08X_2 - 2.58X_3 + 7.22X_1X_2 + 1.08X_1X_3 + 2.74X_2X_3 + 0.11X_1X_2X_3 \quad (9)$$

$$Y_{Cd} = 26.5 + 17.42X_1 + 7.02X_2 - 0.91X_3 + 11.60X_1X_2 - 1.69X_1X_3 + 1.49X_2X_3 - 1.62X_1X_2X_3 \quad (10)$$

Fig. 9. Graphical study of the coefficients values on the extraction of Pr^{3+} and Cd^{2+} to describe the individual and interaction effects of parameters: a_i [pH (2.2 and 11), $[Pr(NO_3)_3] = [CdI_2]$ ($2{\cdot}10^{-4}$ and 10^{-3} mol/L) and w (Magnetic Bentonite) (0.005 and 0.05 g), a_{ij} and a_{ijk} are the constants of the polynomial model [Eqs. (9), (10)].

Table 4
Experimental matrix in coded values and obtained responses

Experiment n^o	Real values			Coded values			Metal uptake	
	X_1	X_2	X_3	X_1	X_2	X_3	$Y_{Pr(III)}$	$Y_{Cd(II)}$
01	2.2	$2{\cdot}10^{-4}$	0.005	–1	–1	–1	55.96	15.9
02	11	10^{-3}	0.005	+1	–1	–1	90.06	27.78
03	2.2	$2{\cdot}10^{-4}$	0.005	–1	+1	–1	32.07	0.59
04	11	10^{-3}	0.005	+1	+1	–1	94.62	65.17
05	2.2	$2{\cdot}10^{-4}$	0.05	–1	–1	+1	43.35	11.23
06	11	10^{-3}	0.05	+1	–1	+1	81.36	22.83
07	2.2	$2{\cdot}10^{-4}$	0.05	–1	+1	+1	30.03	8.39
08	11	10^{-3}	0.05	+1	+1	+1	97.34	59.73
09,10,11	6.6	$6{\cdot}10^{-4}$	0,0275	0	0	0	78.59, 79.75, 79.92	19.01, 20.81, 20.93

Three additional tests at the central point (0, 0, 0) for the calculation of the student's t test.

For the sake of reproducibility, one must check whether this model accurately describes the process investigated by determining which coefficients could be neglected, through Student's t test and Fisher's test [33]. Calculation details are summarized in Table 5.

The model tested at the 95% confidence (i.e., $\alpha = 0.05$), level obtained for extraction of Pr (III) and Cd (II), we assessed the value of $t\nu_{,1-\alpha/2}$ as being equal to 4.3. Therefore, at this (1–α) level, the confidence range for all the coefficients estimated using 08 runs, will be $\Delta a_i = \pm 1.10$ for Praseodymium and $\Delta a_i = \pm 1.63$ for cadmium at 95% confidence. From the Student's t tests, coefficients with $|a_i| < |\Delta a_i|$ must be removed from the mathematical model because they do not show significant effect upon the response function. The resulting new model will be the following:

$$Y_{Pr} = 65.60 + 25.20X_1 - 2.08X_2 - 2.58X_3 + 7.22X_1X_2 + 2.74X_2X_3 \quad (11)$$

$$Y_{Cd} = 26.5 + 17.42X_1 + 7.02X_2 + 11.60X_1X_2 - 1.69X_1X_3 \quad (12)$$

3.8. Interpretation

The effect of individual variables and interactional effects can be estimated from the above equation.

According to Eq. (11), pH of solution has a positive effect, while adsorbent weight and initial concentration have a negative effect, on the praseodymium separation. From Eq. (12), the initial concentration and pH of solution have a positive effect on cadmium adsorption, by adsorp-

Table 5
Model adequacy tests at (0, 0, 0) point and Student's *t* test

Features	Model adequacy for Praseodymium		Model adequacy for Cadmium
	Symbol	Value	Value
Model variance	ν	2	2
Average bleaching capacity at (0,0,0) point	Y0	79.42	20.25
Random variance	S^2	0.52	1.15
Square root of variance	S	0.72	1.07
Risk factor (chosen arbitrary)	α	0.05 (95%)	0.05 (95%)
Student's *t* test factor	$Tv_{1-\alpha/2}$	4.3	4.3
Average error on the coefficient value (trust range)	Δa_i	±1.10 at 95%	±1.63 at 95%
Number of remaining coefficients	R	6	5
Model response at (0,0,0)	a_0 (y_{000})	65.59	26,5
Discrepancy on average yield	d	13.89	6.25
Error on average yield discrepancy	Δd	2.10	±3.13
Average yield for the 8 attempts	Y_m	65.59	26.45
Residual variance	Sr_2	2836.86	1319.84
Degrees of freedom	ν_1	5	4
Residual degrees of freedom	ν_2	2	3
Fisher Test	F	5414.90	1140.94
Fisher-Snedecor law	$F_{a,}\nu_{1,}\nu_2$	$F_{0.95,5,2}$ = 9.33	$F_{0.95,5,2}$ = 9.12

tion in the range of variation of each variable selected for the present study. On the other hand, pH and initial concentration have the greatest effect on both of praseodymium and cadmium separation. A negative value for the effect indicates that the measured value of adsorbed metal amount decreased as the factor was changed from its first level to its second level.

The interaction between pH and initial concentration of praseodymium and cadmium plot in Fig. 10 show a higher separation of praseodymium 95.97% and cadmium 62.41% at the (+1) and (+1) for each factor, a high separation of praseodymium 85.69% and cadmium 25.28% at the (+1) pH and (–1) initial concentration.

As shown earlier in Fig. 11, for the interaction between pH and weight of adsorbent , pH was the most significant parameter witch the interaction at (+1) pH and (–1), (+1) level of adsorbent amount show a high separation of Praseodymium, 93.41 ,88.25% and cadmium 45.56, 42.18% respectively.

The interaction between weight of adsorbent and initial concentration plot in Fig. 11 shows that by increasing or decrease of adsorbent weight, metal separation changes from 62.34, 63.33–73.0%. From Eq. (12) and Fig. 12, the amount of adsorbent is not significant parameter.

✓ For X_1 = +1:

$$Y_{Pr} = 90.80 + 5.14X_2 - 2.58X_3 + 2.74X_2X_3$$

The optimal values are: X_2 = 0.941 and X_3 = –0.854 (Fig. 13a)

✓ For X_1 = –1:

$$Y_{Pr} = 40.4 - 9.3X_2 - 2.58X_3 + 2.74X_2X_3$$

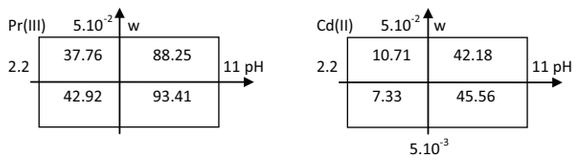

Fig. 10. Factorial interaction between pH and initial concentration of metal ion (X_1X_2).

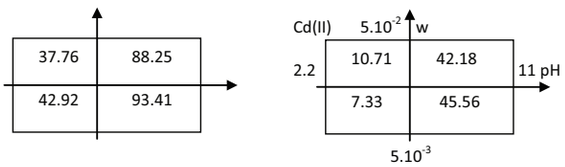

Fig. 11. Factorial interaction between pH and amount of adsorbent (X_1X_3).

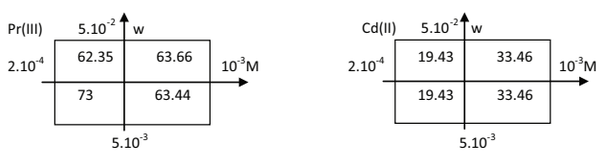

Fig. 12. Factorial interaction between pH and amount of adsorbent (X_2X_3).

The optimal values are: X_2 = 0.941 and X_3 = –0.254 (Fig. 13b)

✓ For X_3 = +1:

$$Y_{Pr} = 40.4 - 9.3X_2 - 2.58X_3 + 2.74X_2X_3$$

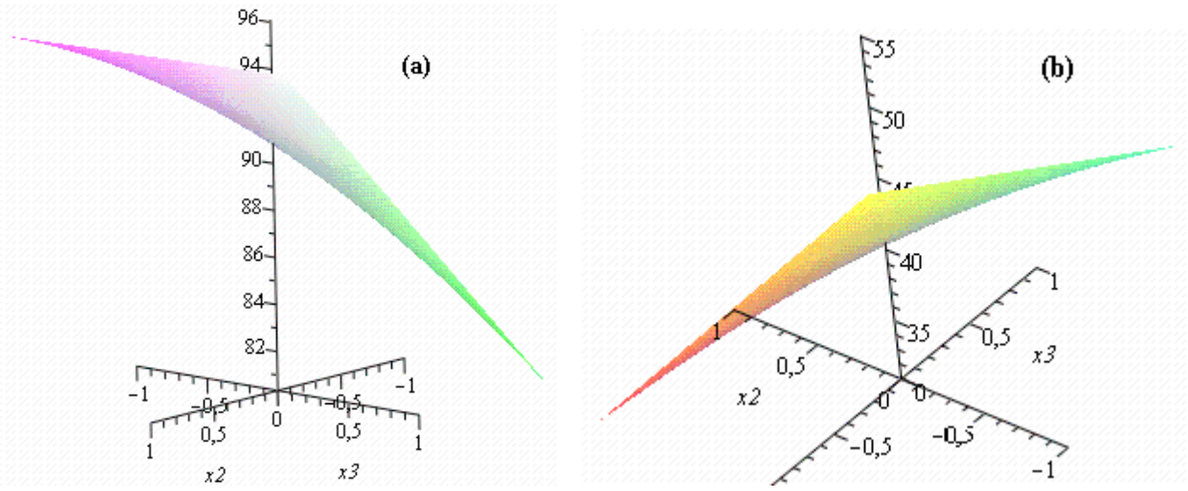

Fig. 13. 3D representation of the Y_{Pr} at fixed $X_1 = +1$ (a) and $X_1 = -1$ (b).

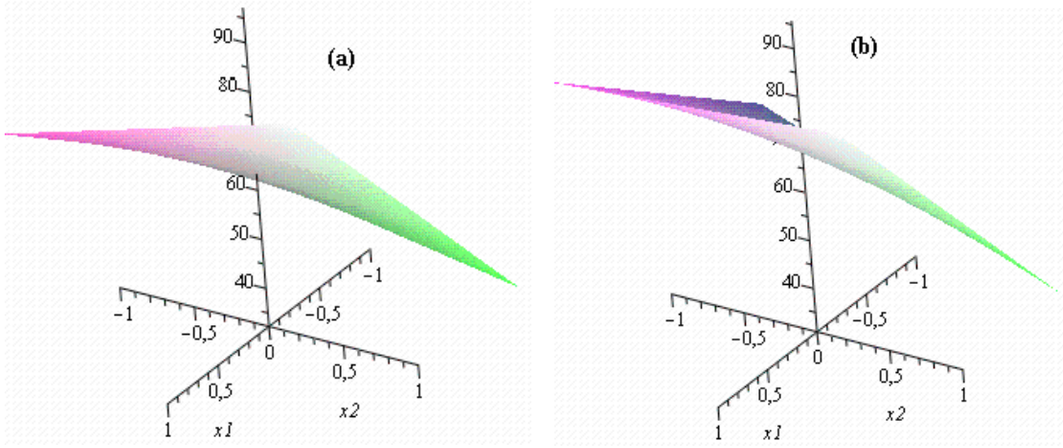

Fig. 14. 3D representation of the Y_{Pr} at fixed $X_3 = +1$ (a) and $X_3 = -1$ (b).

The optimal values are: $X_1 = +0.667$ and $X_2 = -0.954$ (Fig. 14a)

✓ For $X_3 = -1$:

$$Y_{Pr} = 63.02 + 25.20X_1 + 1.66X_2 + 7.22X_1X_2$$

The optimal values are: $X_1 = +0.572$ and $X_2 = -0.754$ (Fig. 14b)

✓ For $X_2 = +1$:

$$Y_{Pr} = 68.18 + 25.20X_1 - 4.82X_2 + 7.22X_1X_2$$

The optimal values are: $X_1 = +0.77$ and $X_3 = -0.554$ (Fig. 15a)

✓ For $X_2 = -1$:

$$Y_{Cd} = 33.52 + 29.02X_1 - 1.69X_1X_3$$

The optimal values are: $X_1 = +0.47$ and $X_2 = -0.854$ (Fig. 15 b)

$$Y_{Cd} = 19.48 + 5.82X_1 - 1.69X_1X_3$$

3.9. Cycle number

For the determination of cycle number, 0.01 g and 0.05 g of magnetic bentonite were used for separation of praseodymium and cadmium. After equilibrium time of 20 min, the same quantities of adsorbent (0.01 g of magnetic bentonite) were added to 5 mL of metal solution 10^{-3} mol·L^{-1}; the maximal extractions 92.80%, 15.64% of praseodymium and cadmium respectively were obtained after six cycles (see Fig. 16a); and with 0.05 g of adsorbent the maximal extractions 90.48%, 15.11% of praseodymium and cadmium respectively (Fig. 16b) were obtained after 2 cycles.

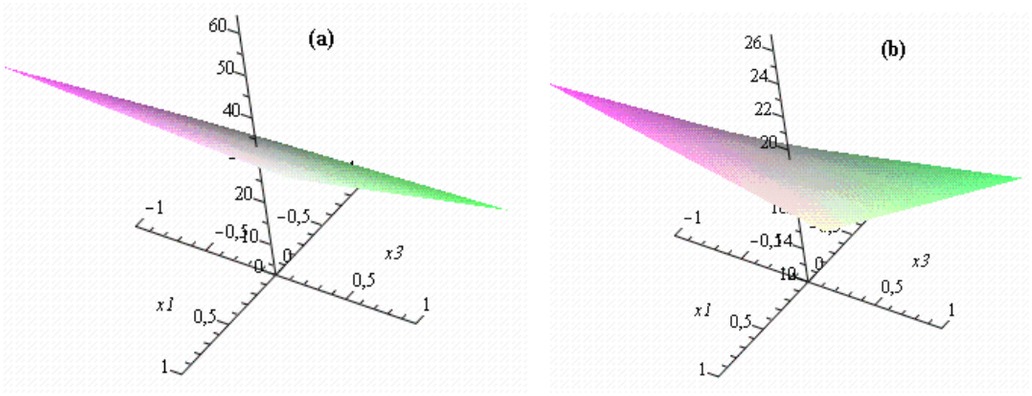

Fig. 15. 3D representation of the Y_{Cd} at fixed X_2 = +1 (a) and X_2= –1 (b).

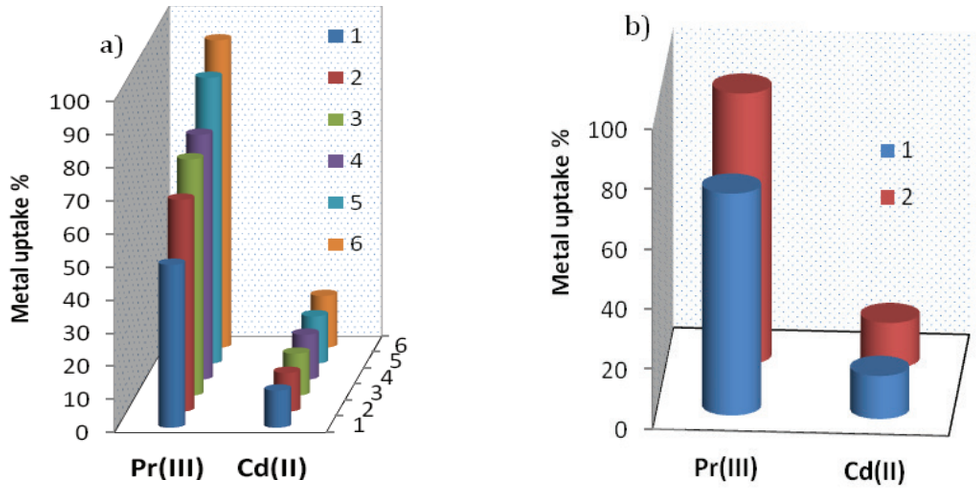

Fig. 16. (a) Cycle number for extraction of metal ions using 0.01 g magnetic bentonite, (b) Cycle number for extraction of metal ions using 0.05 g magnetic bentonite.

4. Conclusions

In this paper, a solid-liquid phase separation of praseodymium and cadmium, using magnetic bentonite, was studied. Proportions of 74.32% and 15.06% of Pr (III) and Cd (II), respectively, were extracted within 20 min at pH 6.5, in one step. The equilibrium data were analyzed using Langmuir, Temkin and Freundlich isotherm models. The results showed that sorption of Pr (III) and Cd (II) had a better fit to Freundlich isotherm model. A 2^3 factorial design was used to study the separation. The pH of the solution together with the combination of the initial pH and concentration were found to be the most significant parameters affecting selectivity. Other interactional parameters also contributed to the increase in the amount of adsorbed metal, though the effect is rather small. Maximum adsorptions of praseodymium and cadmium were determined as 95.32 mg·L^{-1} and 14.36 mg·L^{-1}, respectively. The maximal quantity was 13.2 mg/g for Pr (III) or 33.72 mg/g for $Pr(NO_3)_3$, and 1.47 mg/g for Cd(II) or 4.77mg/g for CdI_2, after six cycles. The maximal quantity was 7.78 mg/g for Pr (III) or 19.72 mg/g for Pr $(NO_3)_3$ and 0.85 mg/g for Cd(II) or 2.77 mg/g for Cd I_2, after two cycles.

These findings confirm the selective adsorption of praseodymium by magnetic bentonite, which indicates that magnetic bentonite is a promising material for selective adsorption, separation and preconcentration.

References

[1] F.H. Spedding, Prologe, in: K.A. Gschneider Jr., L. Eyring (Eds.), Handbook on the Physics and Chemistry of Rare Earths, North-Holland, Amsterdam, 1978, p. XV.
[2] F. An, B. Gao, X. Huang, Y. Zhang, Y. Li, Y. Xu, Z. Chen, J. Gao, Removal of Fe(II) from Ce(III) and Pr(III) rare earth solution using surface imprinted polymer, Desal. Wat. Treat., 51 (2013) 5566–5573.
[3] S.Z. Ajabshir, M.S. Niasari, Preparation and characterization of nanocrystalline praseodymium oxide via a simple precipitation approach, J. Mater. Sci.: Mater. Electron., 26 (2015) 5812–582.
[4] J.S. Varshini, D. Das, N. Das, Optimization of parameters for praseodymium(III) biosorption onto biowaste materials using response surface methodology: Equilibrium, kinetic and regeneration studies, Ecol. Eng., 81 (2015) 321–327.

[5] H. Zhang, J. wang, X. Lu, K. Yang, C. Niu, Effect of praseodymium(III) on zinc(II) species in human interstitial fluid, Biol. Trace Elem. Res., 107(2) (2005) 101–111.
[6] M.H. Mallah, M. Ghannadi Maragheh A. Badiei, R. HabibzadehSbo, Novel functionalized mesopore of SBA-15 as prospective sorbent for praseodymium and lutetium, J. Radioanal. Nucl. Chem., 283 (2010) 597–601.
[7] M. Anitha, D.K. Singh, R. Ruhela, J. Sharma, H. Singh, Studies on the use of octyl (phenyl) phosphinic acid (OPPA) for extraction of yttrium (III) from chloride medium, Desal. Wat. Treat., 38 (2012) 65–72.
[8] N.M. Kozhevnikova, Sorption of praseodymium (III) ions from aqueous solutions by a natural clinoptilolite containing tuff, Zh. Fiz. Khim., 86 (2012) 135–138.
[9] R.K. Kaushal, K.U. Padhyay, Treatability study of low cost adsorbents for heavy metal removal from electro plating industrial effluent: A review, Int. J. Chem. Tech. Res., 6 (2014) 1446–1452.
[10] L. Obeid, A. Bée, D. Talbot, S.B. Jaafar, V. Dupuis, S. Abramson, V. Cabuil, M. Welschbillig, Chitosan/maghemite composite: A magsorbent for the adsorption of methyl orange, Coll. Int. Sci., 410 (2013) 52–58.
[11] C.R. Stela Nhandeyara, A.L.P. Xavier, F.S. Teodoro, M.C. Elias, F.J. Gonc¸ Alves, L.F. Gil, R.P.D Freitas, L.V.A. Gurgel, Modeling mono- and multi-component adsorption of cobalt(II), copper(II), and nickel(II) metal ions from aqueous solution onto a new carboxylated sugar cane bagasse. Part I: Batch adsorption study, Ind. Crops. Prod., 74 (2015) 357–371.
[12] G. Zhao, J. Li, X. Ren, C. Chen, X. Wang, Few-layered graphene oxide nanosheets as superior sorbents for heavy metal ion pollution management, Environ. Sci. Technol., 45 (2011) 10454–10462.
[13] A. Millan, F. Palacio, A. Falqui, E. Snoeck, V. Serin, A. Bhattacharjee, V. Ksenofontov, P. Gutlich, I. Gilbert, Maghemite polymer nanocomposites with modulated magnetic properties, Acta Mater., 55 (2007) 2201–2209.
[14] A.F. Ngomsik, A. Bee, D. Talbot, G. Cote, Magnetic solid–liquid extraction of Eu(III), La(III), Ni(II) and Co(II) with maghemite nanoparticles. Sep. Purif. Technol., 86 (2012) 1–8.
[15] L.C.A. Oliveiraa, R.V.R.A. Rios, J.D. Fabrisa, K. Sapag, V.K. Gargc, R.M. Lago, Clay–iron oxide magnetic composites for the adsorption of contaminants in water, Appl. Clay Sci., 22 (2003) 169–177.
[16] L. Lian, X. Cao, Y. Wu, D. Sun, D. Lou, A green synthesis of magnetic bentonite material and its application for removal of microcystin-LR in water, Appl. Surf. Sci., 289 (2014) 245–251.
[17] B. Makhoukhi, M.A. Didi, H. Moulessehoul, A. Azzouz, D. Villemin, Diphosphonium ion-exchanged montmorillonite for Telon dye removal from aqueous media, Appl. Clay Sci., 50 (2010) 354–361.
[18] T. Shahwan, Ç. Üzüm, A.E. Eroğlu, I. Lieberwirth, Synthesis and characterization of bentonite/iron nanoparticles and their application as adsorbent of cobalt ions, Appl. Clay Sci., 47 (2010) 257–262.
[19] F. Zhao, W.Z. Tang, D. Zhao, Y. Meng, D. Yin, M. Sillanpää, Adsorption kinetics, isotherms and mechanisms of Cd(II), Pb(II), Co(II) and Ni(II) by a modified magnetic polyacrylamide microcomposite adsorbent, Water Proc. Eng., 4 (2014) 47–57.
[20] F.A. Al-Khaldi, B. Abu-Sharkh, A.M. Abulkibash, M.A. Atieh, Cadmium removal by activated carbon, carbon nanotubes, carbon nanofibers, and carbon fly ash: a comparative study, Desal. Wat. Treat., 53(5) (2015) 1417–1429.
[21] N. Chaouch, M.R. Ouahrani, S. Chaouch, N. Gherraf, Adsorption of cadmium (II) from aqueous solutions by activated carbon produced from Algerian dates stones of Phoenix dactylifera by H_3PO_4 activation, Desal. Wat. Treat., 51 (2013) 2087–2092.
[22] A. Idris, N. Ismail, N. Hassan, E. Misran, A. Ngomsik, Synthesis of magnetic alginate beads based on maghemite nanoparticles for Pb(II) removal in aqueous solution, J. Ind. Eng. Chem., 18 (2012) 1582–1589.
[23] J.M.D. Coey, J.W. Stucki, B.A. Goodmann, U. Schwertmann, Magnetic properties of iron in soil iron oxides and clay minerals, D. Reidel, (1988) 397–466.
[24] B. Makhoukhi, M. Djab, M.A. Didi, Adsorption of Telon dyes onto bis-imidazolium modified bentonite in aqueous solutions, Env. Chem. Eng., 3 (2015) 1384–1392.
[25] X. He, R. Che, Y. Wang, Y. Li, L. Wan, X. Xiang, Core–nanoshell magnetic composite material for adsorption of Pb(II) in wastewater, Env. Chem. Eng., 3 (2015) 1720–1724.
[26] M.P. Gatabi, H.M. Moghaddam, M. Ghorbani, Point of zero charge of maghemite decorated multiwalled carbon nanotubes fabricated by chemical precipitation method, J. Mol. Liq., 216, 117–125.
[27] I. Puigdomenech, (2006) HYDRA (Hydrochemical Equilibrium-Constant Database) and MEDUSA (Make Equilibrium Diagrams Using Sophisticated Algorithms) Programs. Royal Institute of Technology, Stockholm. http://www.kemi.kth.se/medusa/
[28] S. Bao, L. Tang, K. Li, P. Ning, J. Peng, H. Guo, T. Zhu, Y. Liu, Highly selective removal of Zn(II) ion from hot-dip galvanizing pickling waste with amino-functionalized Fe_3O_4@SiO_2 magnetic nano-adsorbent, J. Colloid Interface Sci., 462 (2016) 235–242.
[29] W. Jiang, M. Pelaez, D. Dionysiou, M.H. Entezari, D. Tsoutsou, K. O'Shea, Chromium(VI) removal by maghemite nanoparticles, Chem. Eng. J., 222 (2013) 527–533.
[30] E.A. El-Sofany, Separation of praseodymium from aqueous nitrate medium by inorganic exchanger, Int. J. Ecosyst. Ecol. Sci., 2(2) (2011) 149–162.
[31] F. Geyikçi, H. Büyükgüngör, Factorial experimental design for adsorption silver ions from water onto montmorillonite, Acta. Geodyn. Geomater., 10(3) (2013) 363–370.
[32] A. Amara-Rekkab, M.A. Didi, Design optimization of extraction procedure for mercury (II) using Chelex 100 resin, Desal. Wat. Treat., 57(15) (2016) 6950–6958.
[33] M.A. Didi, B. Makhoukhi, A. Azzouz, D. Villemin, Colza oil bleaching through optimized acid activation of bentonite, Appl. Clay Sci., 42 (2009) 336–344.